MULTIMODAL OPTICAL COHERENCE TOMOGRAPHY IN THE ASSESSMENT OF CANCER TREATMENT EFFICACY

Sirotkina MA[1] ✉, Kiseleva EB[1], Gubarkova EV[1], Buyanova NL[1], Elagin VV[1], Zaitsev VYu[1,2], Matveev LA[1,2], Matveev AL[1,2], Kirillin MYu[2], Gelikonov GV[1,2], Gelikonov VM[1,2], Kuznetsov SS[1], Zagaynova EV[1], Gladkova ND[1]

[1] Nizhny Novgorod State Medical Academy, Nizhny Novgorod, Russia

[2] Institute of Applied Physics, Russian Academy of Sciences, Nizhny Novgorod, Russia

One of the challenges faced by modern medicine is finding new methods of functional imaging of biological tissues in patients that allow detection of early tumor response to treatment. One of such methods proposed in this work is multimodal optical coherence tomography (MM OCT). It combines cross-polarization OCT (CP OCT) for visualization of tissue structure and assessment of connective tissue health, OCT-based microangiography (OCT MA) for visualization of the vasculature, and OCT-based elastography for measuring tissue stiffness. The efficacy of this method was tested during the course of photodynamic therapy (PDT), as major PDT targets are cellular and vascular components of a tumor. The experiments were carried out on the CT26 colon carcinoma transplanted into the mouse ear. It was shown that the efficacy of PDT can be assessed using MM OCT. For example, CP OCT can help differentiate between necrotic and intact tumors; OCT MA detects blood circulation defects that lead to slower blood circulation or circulatory stagnation followed by tumor death. OCT-based elastography is helpful in assessing stiffness of normal and pathological tissues.

Keywords: multimodal optical coherence tomography, cross-scattering, microangiography, elastography, photodynamic therapy, CT26 colon carcinoma, experimental tumor

Funding: this work was supported by the Ministry of Education and Science of the Russian Federation (grant no. 14.B25.31.0015), numerical processing of CP OCT images was supported by grant no. 15-32-20250 of the Russian Foundation for Basic Research, algorithm modification and development of software/hardware OCT-system for mapping microcirculation and elastography images was supported by the grant of the President of the Russian Federation for young scientists (no. MK-6504.2016.2) and the grant of the Russian Foundation for Basic Research (no. 16-02-00642-a).

Acknowledgements: authors thank professor Alex Vitkin of University of Toronto (Toronto, Canada), the leading scientist of the Russian Federation Government Mega-grant 14.B25.31.0015.

✉ **Correspondence should be addressed:** Marina Sirotkina
pl. Minina i Pozharskogo, d. 10/1, Nizhny Novgorod, Russia, 603950; sirotkina_m@mail.ru

Recieved: 15.08.2016 **Accepted:** 25.08.2016

ПРИМЕНЕНИЕ МУЛЬТИМОДАЛЬНОЙ ОПТИЧЕСКОЙ КОГЕРЕНТНОЙ ТОМОГРАФИИ В ОЦЕНКЕ ЭФФЕКТИВНОСТИ ТЕРАПИИ РАКА

М. А. Сироткина[1] ✉, Е. Б. Киселева[1], Е. В. Губарькова[1], Н. Л. Буянова[1], В. В. Елагин[1], В. Ю. Зайцев[1,2], Л. А. Матвеев[1,2], А. Л. Матвеев[1,2], М. Ю. Кириллин[2], Г. В. Геликонов[1,2], В. М. Геликонов[1,2], С. С. Кузнецов[1], Е. В. Загайнова[1], Н. Д. Гладкова[1]

[1] Нижегородская государственная медицинская академия, Нижний Новгород

[2] Институт прикладной физики РАН, Нижний Новгород

Поиск новых способов прижизненной функциональной визуализации биологических тканей, которые позволяют выявлять ранний ответ опухоли на выбранную терапию с целью коррекции курса лечения, — актуальная задача современной медицины. В качестве такого способа в работе предложена мультимодальная оптическая когерентная томография (ММ ОКТ), которая сочетает в себе кросс-поляризационную ОКТ (КП ОКТ) для визуализации структуры ткани и оценки состояния соединительнотканного компонента, ОКТ-микроангиографию (ОКТ МА) для визуализации сосудистого русла и ОКТ-эластографию для изучения жесткости ткани. Эффективность метода проверяли на примере действия фотодинамической терапии (ФДТ), поскольку основными мишенями ФДТ являются клеточный и сосудистый компоненты опухоли. В качестве объекта исследования была выбрана карцинома кишечника мыши CT26, локализованная на ухе мыши. Показано, что с помощью ММ ОКТ можно оценить эффективность ФДТ, а именно: по КП ОКТ — отличить опухоль с некрозом от интактной опухоли, по ОКТ МА — выявить расстройства кровообращения, приводящие к замедлению или остановке кровотока и дальнейшей гибели опухоли, а по ОКТ-эластографии — определить жесткость нормальной и патологической ткани.

Ключевые слова: мультимодальная оптическая когерентная томография, кросс-рассеяние, микроангиография, эластография, фотодинамическая терапия, карцинома кишечника CT26, экспериментальная опухоль

Финансирование: работа выполнена при финансовой поддержке гранта Министерства образования и науки РФ (договор № 14.B25.31.0015); числовая обработка КП ОКТ-изображений поддержана грантом Российского фонда фундаментальных исследований (проект № 15-32-20250); модификация алгоритма и разработка программно-аппаратного ОКТ-комплекса для картирования микроциркуляторных и эластографических изображений поддержана грантом Президента РФ для молодых ученых № МК-6504.2016.2 и грантом Российского фонда фундаментальных исследований № 16-02-00642-а.

Благодарности: авторы благодарят профессора Алекса Виткина из Университета Торонто (Торонто, Канада) — ведущего ученого мегагранта, в рамках которого выполнена работа.

✉ **Для корреспонденции:** Сироткина Марина Александровна
603950, г. Нижний Новгород, пл. Минина и Пожарского, д. 10/1; sirotkina_m@mail.ru

Статья получена: 15.08.2016 **Статья принята в печать:** 25.08.2016

In spite of advances in the diagnosis and treatment of cancer, mortality in cancer patients is still high. Tumor heterogeneity remains a challenge that largely affects treatment progress [1]. Patients with tumors of the same type often respond differently to identical therapies. Thus, detecting early tumor response to treatment is crucial for introducing timely adjustments to a treatment plan. The literature reports studies aimed at finding criteria for the assessment of antitumor therapy efficacy [2], but no reliable models have been suggested so far.

Optical coherence tomography (OCT) is a noninvasive diagnostic tool for imaging in turbid media. OCT utilizes backscattering, permitting scan depth of 1–2 mm, and forms 2D and 3D images. This technique is based on the low coherence interferometry with a broad bandwidth light source in the near-infrared wavelength range (the so-called therapeutic transparency window of 0.7–1.3 μm) [3–5]. OCT is not damaging to the organism, since its power output is only 3–5 mW. Compared to nuclear magnetic resonance imaging and high frequency ultrasound scanning, it has a higher spatial resolution (up to 15 μm), is more cost-effective and easier to use. Clinically, it is used for early diagnosis of neoplasia, resection margin definition prior to excision and for monitoring patients with previous cancers in order to timely detect recurrences [6].

The application of this technique is not limited to standard tissue visualization. It can also be used for blood circulation and vasculature structure imaging. It is very important for biological and medical research, as it allows obtaining data on tissue functioning *in vivo*. Such data can influence the choice of cancer therapy, as some treatments induce vascular damage in tumors [7]. Therefore, a lot of research laboratories are now working on optimizing OCT techniques for intravital microvascular imaging. Among the most promising methods of detection, visualization and quantitative assessment/monitoring of tissue microcirculation are those based on speckle variance [8].

Mechanical properties of biological tissues are related to their structure and functions that change in the presence of pathology or during the course of treatment. The last 15 years have seen the increasing focus on OCT-based tissue stiffness measuring (tissue elasticity mapping). Optical coherence elastogrpahy has been demonstrated *in vivo* [9] and recommended for tumor detection in soft tissues [10]. Some researchers have described the potential of this method for differentiating between malignant and healthy breast tissues [14, 15]. At the moment, there are no OCT scanners for elastographic mapping on the market. In Russia, there are a number of research centers in Nizhniy Novgorod, Saratov and St. Petersburg that work on OCT optimization, but only a few researchers from the Institute of Applied Physics of RAS (Nizhny Novgorod) and Nizhny Novgorod State Medical Academy (NNSMA) work with optical coherence elastogrpahy [16].

A combination of the methods described above forms a multimodal OCT that can be an effective tool for monitoring tumor response to therapy and interpreting new findings, thus driving us toward personalized treatment. The aim of this work was to test the feasibility of three OCT modalities for the assessment of tumor response to therapy.

METHODS

Animal model

The study was carried out on the experimental model of murine CT26 colon carcinoma. The tumor cell suspension (200,000 cells in 20 μl phosphate buffer) was inoculated intracutaneously into the external auricle tissue of 8-month old female BALB/c mice (weight of 20–22 g). An ear tumor model is characterized by a surface growth, a relatively small size (several millimeters in diameter) and good accessibility for visual examination and optical bioimaging. The experiment was approved by the Ethics Committee of NNSMA (protocol no. 14 dated December 10, 2013).

Photodynamic therapy

We decided on the short-term (from several hours up to several days) photodynamic therapy (PDT) that affects both vascular and cellular tumor components. PTD was introduced 10–14 days after the inoculation when the tumor size was 3.5–4.0 mm and its vasculature was well formed. The animals received 5 mg/kg i. v. Fotoditazin by Veta-Grand, Russia. One hour after the photosensitizer injection, the tumor was exposed to the diode laser radiation with a wavelength of 659 nm; the dosage used was 75 J/cm2 (100 mW/cm^2). The experimental group consisted of 10 animals; the control group included 5 mice.

Multimodal optical coherence tomography

The tumor response to PDT was assessed by MM OCT using the system developed by the Institute of Applied Physics, RAS. System parameters were as follows: operating wavelength of 1.3 μm, power output of 15 mW, transverse spatial resolution of 25 μm, axial resolution of 15 μm, scanning depth of up to 1.7 μm. Probing radiation was circularly polarized, scanning speed was 20,000 A-scans per second.

We performed noncontact MM OCT scanning by positioning the optical probe at 1.5 cm distance from the studied surface.

2D images (B-scans) of 4 × 4 mm were obtained in the cross-polarization OCT (CP OCT) mode. The scans consisted of 2 pseudocolor images: the top co-polarized image showing the intensity of backscattered waves that preserved the initial level of polarization, and the bottom cross-polarized image showing the intensity of backscattered waves that changed their initial polarization to orthogonal. In most cases, cross-scattering is observed in highly organized anisotropic structures, such as collagen and elastic fibers [17]. The CP OCT mode allows recording 3D images in co- and cross-polarization modes, each of them of 4 × 4 × 2 mm in size (the figures correspond to planar dimensions and depth).

Quantitative processing of CP OCT images included computing of the integral depolarization factor (IDF) for the manually selected area of interest (selection was based on histological analysis results and qualitative attributes of CP OCT images). IDF calculation algorithm was previously developed by the authors of this work and described in [18]. We had used it for the assessment of the functional state of collagen fibers in various tissues (bladder and oral mucosa, aorta and coronary arteries). Its calculation is based on the averaged ratio of OCT signal intensities in cross- and co-polarization modes.

Tissue stiffness was assessed using optical coherence elastogrpahy. To extract information from the OCT signal, we used an improved (hybrid) phase-sensitive approach to strain estimation [16]. The probe was slightly pressed to the studied surface (a tissue compression method used for data acquisition), and the deformities in the probe vicinity were registered. Elastographic mapping is based on the analysis of spatial heterogeneity of changes in the OCT signal phase in the tissue induced by its motion. On the resulting pseudocolor images, stiffer areas (those with little deformation) are shown in blue, and soft areas, where deformation is considerable, are shown in red.

The microvasculature was studied using OCT-based microangiography (OCT MA). Vascular network visualization is based on the time-related alterations of OCT signal amplitude and phase shown on the series of pixelated OCT images of the same tissue region. The areas where the signal changes rapidly indicate the presence of flowing liquid (blood). The areas of pixels with stable values of amplitudes and phases mean there is no liquid there. Thus, OCT MA can be used for the visualization of both normal blood circulation and stasis, as in PDT-induced thrombosis. OCT MA scans were obtained from the area of 2 x 2 mm^3. The pattern was highly sensitive making it possible to visualize small blood vessels. Processed OCT MA images were a projection of the maximum signal intensity (a vascular network top view, full depth imaging) [19].

Fluorescence microscopy

The data on the vascular network structure obtained with OCT MA were verified by fluorescence microscopy on the Axio Zoom.V16 stereomicroscope (Zeiss, Germany) using FITC fluorophore conjugated to dextran (Sigma-Aldrich, USA). 50 mg/kg fluorophore were injected i. v. into the tail vein. Images were obtained within 10 minutes after fluorophore administration.

Histological analysis

Tumor cell death and blood circulation defects were verified by light microscopy 2 days after PDT. Samples were fixated in 10 % neutral buffered formalin. 7 μm thick histological sections were prepared using the Leica SM 2000 R sliding microtome (Leica Biosystems, Germany). To study tumor tissue morphology, the sections were deparaffinized and stained with hematoxylin and eosin.

RESULTS

MM OCT imaging of mouse ear tissue

CP OCT

Ear tissue is a layered structure consisting of the epidermis, the dermis with cutaneous appendages, and the cartilage (fig. 1A). In the co-polarization mode, CP OCT images of healthy ear tissue show a layered structure with the cartilage in the middle represented as a thin line of a low intensity signal; on the both sides of it are dermis layers of a high intensity signal. The epidermis is visualized above the dermis as a very thin line of a low intensity signal (fig. 1B). In the cross-polarization mode, the image is also layered, but the signal intensity of the co-polarized layers described above is an order of magnitude weaker, because this mode can only "see" a signal from optically anisotropic structures, such as collagen or elastic fibers of the dermis and the cartilage. As the tumor grows in the dermis, the total volume of the tissue above the cartilage gradually increases, and CP OCT scans show deformation of tissue layers. Images obtained by noncontact scanning show a small protuberance in the tumor site (fig. 1D). Dense tumor cells do not cross-polarize or cross-scatter the probing radiation. The signal intensity around the tumor is reduced due to the disrupted organization of dermal collagen (fig. 1D).

OCT MA

OCT MA was used to visualize the structure of the vascular network of healthy ear tissues (fig. 2B) and the area where the CT26 tumor had been transplanted (fig. 2G). Images of normal tissue show large blood vessels, i. e., arterioles and venules. In the presence of pathology, smaller blood vessels can be visualized forming a dense interwoven network. Such imaging specifics can be related to the formation of new blood vessels in the tumor or to the increased blood flow velocity in the already existing vessels. We are still working on the interpretation of this fact. The vascular network structures in healthy and pathological tissues visualized on OCT MA images are identical to those seen on fluorescence microscopy images (fig. 2C, 2E), which indicates that data obtained with OCT MA are accurate. Thus, OCT MA can be used to differentiate between normal and pathological tissues.

Optical coherence elastography

Examples of *in vivo* elastographic deformation mapping in lab animals using manual probing are presented in fig. 3. Fig. 3A and 3B show structured and elastographic images of healthy ear tissue. The structured image (fig. 3A) shows that tissue in the selected frame is morphologically heterogenic and the OCT signal is scattered evenly; as a result, the elastographic map reflects uniform strain distribution (fig. 3B). The same area looks 2.0–2.5 times thicker in the structured image of the ear tissue sample with the transplanted tumor (fig. 3C) and is characterized by reduced scattering of probing signal. The elastographic map (fig. 3G) shows that tumor site is presented as a clearly outlined deformation zone.

CT26 tumor growth in the mouse ear

CT26 tumor growth was studied using CP OCT and OCT MA. As the tumor grows, the CP OCT images demonstrate that signal intensity drops and reaches its minimum on day 14 after tumor inoculation. The signal penetration depth also decreases (fig. 4, top row). OCT MA images show that as the tumor grows in size, the number of blood vessels also increases (fig. 4, bottom row).

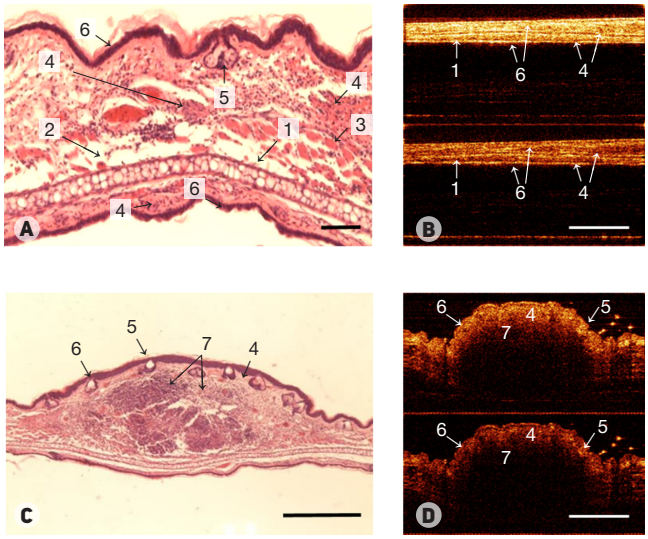

Fig. 1. Visualization of healthy tissue **(A, B)** and CT26 colon carcinoma transplanted into the mouse ear **(C, D)**

(A) and **(C)** are histological sections (the scale bars are 100 μm and 500 μm, respectively). **(B)** and **(D)** are images obtained with cross-polarized optical coherence tomography (the scale bar is 1 μm). 1 — the cartilage; 2 — the adipocyte layer; 3 — the cross-striated muscle; 4 — the dermis; 5 — hair follicles; 6 — the epidermis; 7 — the tumor tissue.

Tumor response to photodynamic treatment

Analysis of histological sections

PDT causes damage to malignant cells and disrupts blood flow to the tumor. On day 2 after the treatment necrotic lesions were detected covering about 60 % of the whole tumor. Along with tissue necrosis, we observed blood circulation defects: stasis, sludge syndrome, thrombosis and hemorrhage.

Analysis of CP OCT images

The damaging effect of PDT on tumor cells and vasculature is supposed to affect optical properties of the tumor. Fig. 5 shows depolarization factor maps for the experimental (PDT) and control groups. In the controls, the tumor was characterized by low values of depolarization factor (fig. 5A) suggesting low cross-scattering capacity of the tissue. In tumors treated with PDT, IDF maps show increased cross-scattering (fig. 5B): IDF values increase from 0.020 ± 0.007 to 0.036 ± 0.013. We conclude that prevalence of necrotic lesions in the tumor formed by the deposition of inflammatory cells, destroyed collagen fibers and true tumor cells leads to the increased number of cross-scatter sites and a higher IDF.

Analysis of OCT MA images

OCT MA-based monitoring of the tumor vascular network within a few hours after the treatment demonstrates the instant response of the vasculature to radiation: the majority of blood vessels are not visualized during the procedure (fig. 6B). 24 h after PDT, the vessels are not visualized on OCT MA (fig. 6C). The obtained results confirm that in the presence of blood circulation abnormalities that significantly reduce blood flow or cause stasis, OCT MA does not visualize blood vessels. Fluorescence microscopy images also do not show the vascular network (fig. 6E).

DISCUSSION

In this work, we present the results of the first multimodal OCT-based complex study of normal and pathological tissues. We obtained and analyzed OCT images of tissue structure and vascular network and maps of stiffness distribution

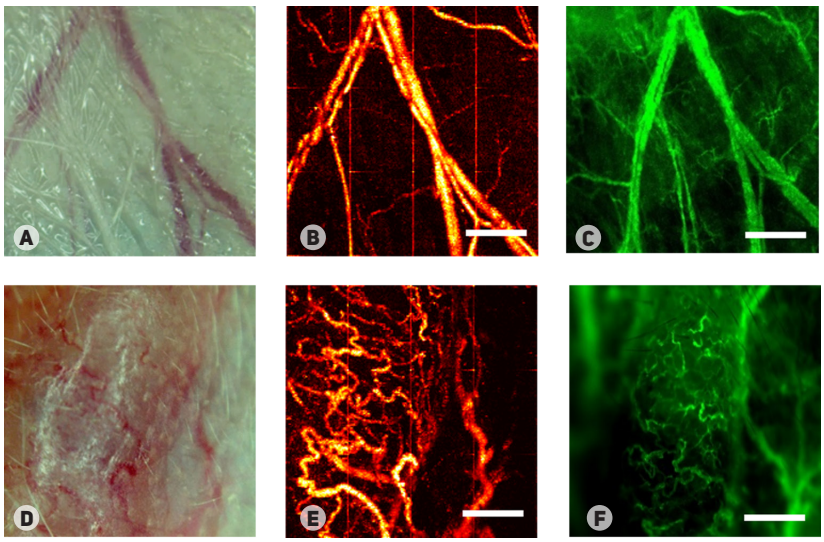

Fig. 2. Visualization of a vascular network of healthy tissue **(A–C)** and CT26 colon carcinoma transplanted into the mouse ear **(D–F)**
(A) and **(B)** are microphotographs, **(C)** and **(D)** are images obtained with OCT-based microangiography, **(E)** and **(F)** are fluorescence microscopy images. The scale bar is 0.5 mm.

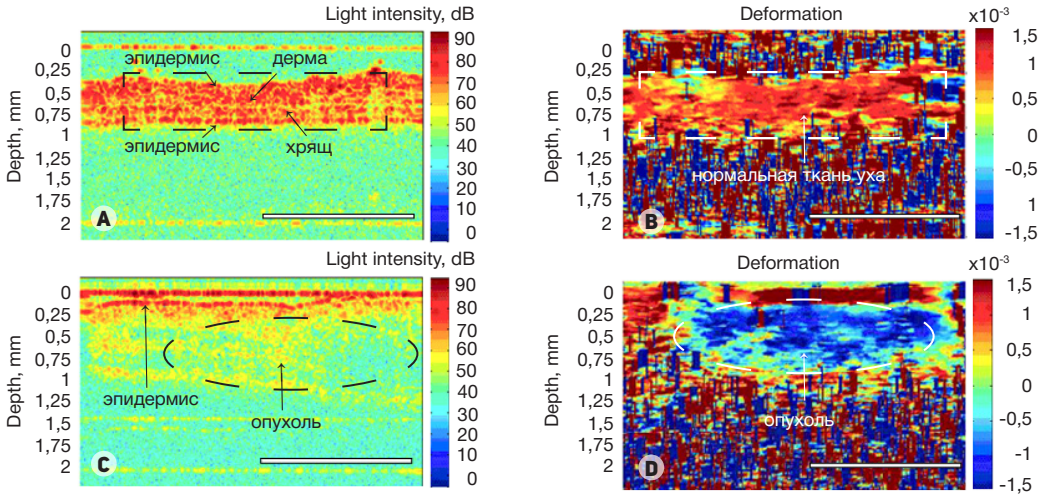

Fig. 3. Structured *in vivo* OCT images **(A, C)** and elastographic deformation maps **(B, D)** of healthy tissues of the mouse ear **(A, B)** and CT26 colon carcinoma transplanted into the mouse ear **(C, D)** (the scale bar is 1 mm)

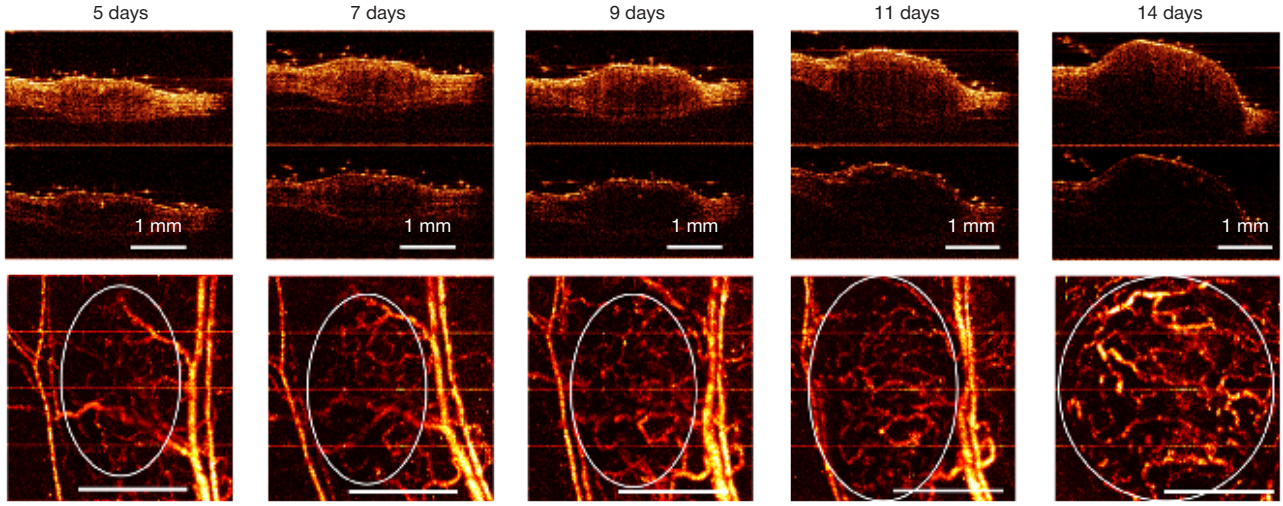

Fig. 4. MM OCT-based monitoring of CT26 colon carcinoma transplanted into the mouse ear
Top row: CP OCT images; bottom row: OCT MA images. The tumor site is circled.

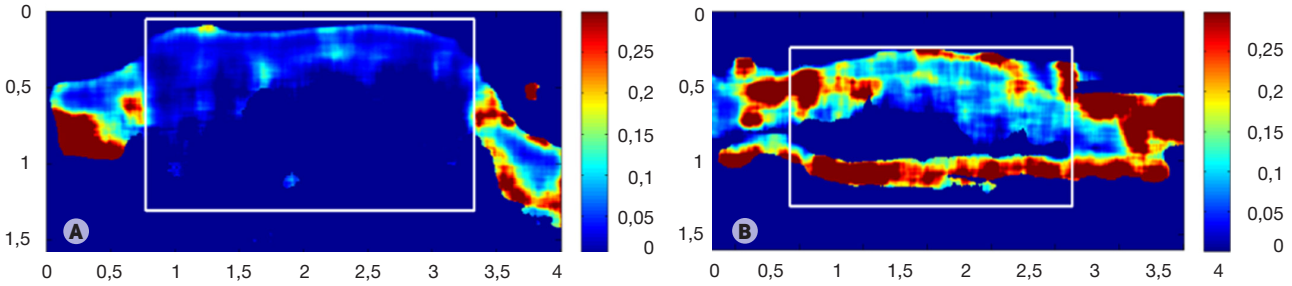

Fig. 5. Depolarization maps based on B-scans. **(A)** — tumor before photodynamic therapy, **(B)** — tumor after photodynamic therapy

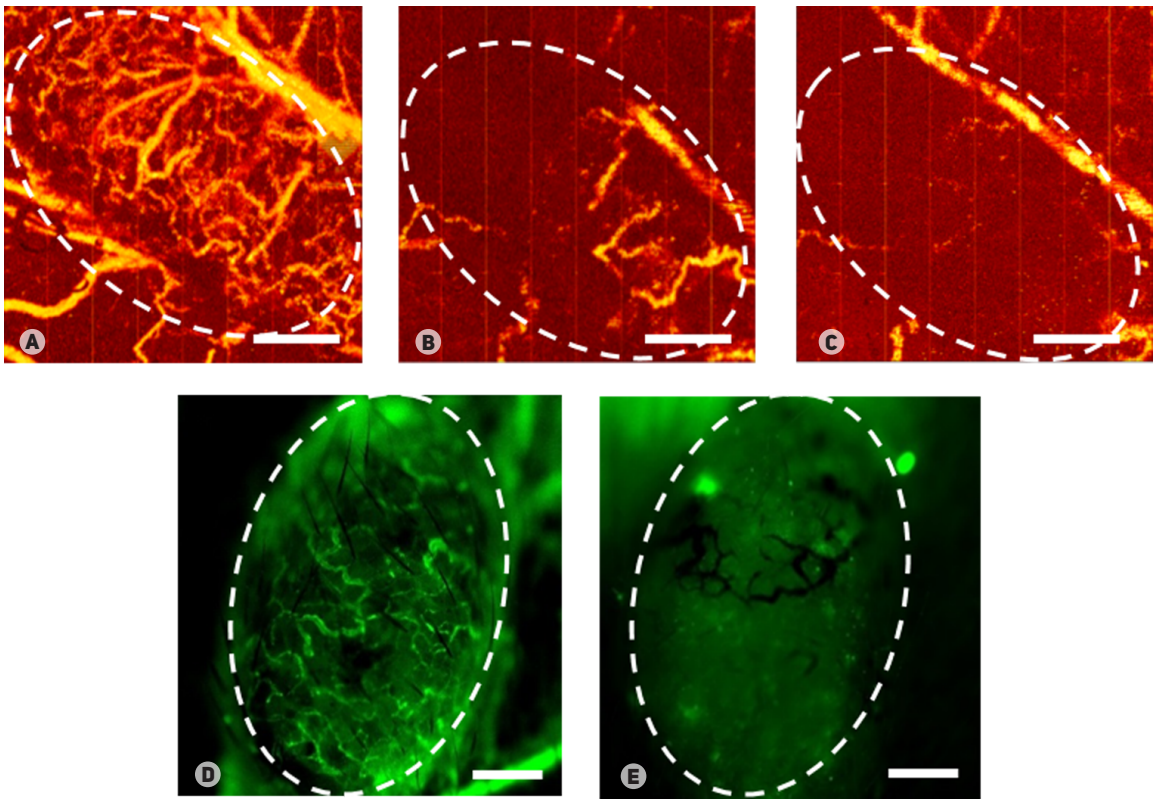

Fig. 6. Visualization of the vascular response of CT26 colon carcinoma transplanted into the mouse ear to photodynamic therapy on OCT MA **(A–C)** and fluorescence microscopy **(D, E)**. **(A)** and **(D)** — before treatment, **(B)** — immediately after treatment, **(C)** and **(E)** — 24 h after treatment. The scale bar is 0.5 mm. The tumor site is marked with a dotted circle

(elastographic OCT images). A possibility of using MM OCT for the assessment of antitumor treatment was demonstrated convincingly. Other researchers explore isolated OCT modalities. For example, optical coherence elastography and its application in ophthalmology have been studied in the USA since 2000 [14, 15, 20, 21]. The leading positions in this area of research are held by the Australian team of D. Sampson [12, 22]. An outstanding contribution to the improvement of OCT-based visualization of tissue microcirculation (capillary vessels, in particular) has been made by the research groups headed by M. Leahy [23], R. Wang [24] and A. Vitkin [25]. Vascular response to PDT has also been studied [26, 27].

At the moment, OCT is a verified method for visual assessment of structural changes in skin cancers treated with PDT and a follow-up tool for monitoring tumor margins [28, 29]. However, certain changes in the tumor cell profile registered on OCT images are not visible to the unaided eye; here, quantitative assessment of OCT images can be more reliable. This approach has largely contributed to the diagnosis accuracy [18]. IDF calculation for the assessment of tumor response to PDT helps to accurately analyze the obtained images, describe the underlying mechanism of tumor cell death and stroma degradation and understand the role of inflammatory cells in this process.

MM OCT monitoring of tumor growth detected gradual development of the vascular network in the tumor. Apparently, the degree of tumor vascularization can influence the choice of treatment plan: in well vascularized tumors the photosensitizer will accumulate in larger concentrations, and such tumors can be successfully destroyed with PDT that affects the vasculature.
We have demonstrated that simultaneous use of three OCT modalities in tumor studies provides information on both the structure of tissue consisting of collagen fibers and blood vessels and its stiffness. Altogether, these data are important for the accurate assessment of tumor response to therapy. We believe that particular focus should be drawn to studying the tumor prior to treatment, as initial imaging results can influence the choice of treatment strategy. For example, poorly vascularized tumors are most likely hypoxic; here, radiation or PDT will be ineffective, chemotherapy drugs will not accumulate in the tumor properly, and targeted delivery of medication will be required.

CONCLUSIONS

We have demonstrated the potential of multimodal optical coherence tomography as a basis for the personalized antitumor treatment using photodynamic therapy as an example. Based on the analysis of scattering and polarizing properties of tissues, CP OCT provides data on tissue structure and collagen fibers and detects necrotic lesions in the tumor. OCT MA allows real time visualization of the vasculature in normal and tumor tissues and can be used to assess the functional state of blood vessels. Observing the response of tumor vasculature to treatment right after its completion allows for the adjustments to the treatment plan in case the vascular response is absent. We have tested a novel robust method of obtaining elastographic images that can be employed to generate deformation maps in vivo using manual probing, which is highly important for clinical studies. The complex assessment of tissues based on MM OCT is a huge step towards personalized treatment of cancers.

References

1. Casas A, Di Venosa G, Hasan T, Al Batlle. Mechanisms of resistance to photodynamic therapy. Curr Med Chem. 2011; 18 (16): 2486–515.
2. Mallidi S, Watanabe K, Timerman D, Schoenfeld D, Hasan T. Prediction of Tumor Recurrence and Therapy Monitoring Using Ultrasound-Guided Photoacoustic Imaging. Theranostics. 2015 Jan 1; 5 (3): 289–301.
3. Huang D, Swanson EA, Lin CP, Schuman S, Stinson WG, Chang W, et al. Optical coherence tomography. Science. 1991 Nov 22; 254 (5035): 1178–81.
4. Schmitt JM, Xiang SH. Cross-polarized backscatter in optical coherence tomography of biological tissue. Opt Lett. 1998 Jul 1; 23 (13): 1060–2.
5. Bouma BE, Tearney GJ. Clinical imaging with optical coherence tomography. Acad Radiol. 2002 Aug; 9 (8): 942–53.
6. Zagaynova EV, Gladkova ND, Shakhova NM, Streltsova OS, Kuznetsova IA, Yanvareva IA, et al. Optical Coherence Tomography Monitoring of Surgery in Oncology. In: Popp J, Tuchin V, Chiou A, Heinemann SH, editors. Handbook of Biophotonics. Wiley-VCH; 2012. p. 337–76.
7. Enfield J, Jonathan E, Leahy M. In vivo imaging of the microcirculation of the volar forearm using correlation mapping optical coherence tomography (cmOCT). Biomed Opt Express. 2011; 2 (5): 1184–93.
8. Mariampillai A, Leung MK, Jarvi M, Standish BA, Lee K, Wilson BC, et al. Optimized speckle variance OCT imaging of microvasculature. Opt Lett. 2010; 35 (8): 1257–9.
9. Kennedy BF, Hillman TR, McLaughlin RA, Quirk BC, Sampson DD. In vivo dynamic optical coherence elastography using a ring actuator. Opt Express. 2009; 17 (24): 21762–72.
10. Wang S, Li J, Manapuram RK, Menodiado FM, Ingram DR, Twa MD, et al. Noncontact measurement of elasticity for the detection of soft-tissue tumors using phase-sensitive optical coherence tomography combined with a focused air-puff system. Opt Lett. 2012; 37 (24): 5184–6.
11. Srivastava A, Verma Y, Rao K, Gupta P. Determination of elastic properties of resected human breast tissue samples using optical coherence tomographic elastography. Strain. 2011; Feb 1; 47 (1): 75–87.
12. Kennedy KM, McLaughlin RA, Kennedy BF, Tien A, Latham B, Saunders CM, et al. Needle optical coherence elastography for the measurement of microscale mechanical contrast deep within human breast tissues. J Biomed Opt. 2013; 18 (12): 121510.
13. Kennedy BF, McLaughlin RA, Kennedy KM, Chin L, Wijesinghe P, Curatolo A, et al. Investigation of Optical Coherence Micro-elastography as a Method to Visualize Cancers in Human Breast Tissue. Cancer Res. 2015; 75 (16): 3236–45.
14. Wang S, Larin KV, Li J, Vantipalli S, Manapuram RK, Aglyamov S, et al. A focused air-pulse system for optical-coherence-tomography-based measurements of tissue elasticity. Laser Physics Letters. 2013; 10 (7): 075605.
15. Nguyen TM, Song S, Arnal B, Wong EY, Huang Z, Wang RK, et al. Shear wave pulse compression for dynamic elastography using phase-sensitive optical coherence tomography. J Biomed Opt. 2014; 19 (1): 016013.
16. Zaitsev VY, Matveyev AL, Matveev LA, Gelikonov GV, Gubarkova EV, Gladkova ND, et al. Hybrid method of strain estimation in optical coherence elastography using combined sub-wavelength phase measurements and supra-pixel displacement tracking. J Biophotonics. 2016; 9 (5): 499–509.
17. Gubarkova EV, Dudenkova VV, Feldchtein FI, Timofeeva LB, Kiseleva EB, Kuznetsov SS, et al. Multi-modal optical imaging characterization of atherosclerotic plaques. J Biophotonics. 2015 Nov 25. doi: 10.1002/jbio.201500223.

18. Kiseleva E, Kirillin M, Feldchtein F, Vitkin A, Sergeeva E, Zagaynova E, et al. Differential diagnosis of human bladder mucosa pathologies in vivo with cross-polarization optical coherence tomography. Biomed Opt Express. 2015; Apr 1; 6 (4): 1464–76.
19. Matveev LA, Zaitsev VYu, Gelikonov GV, Matveyev AL, Moiseev AA, Ksenofontov SYu, et al. Hybrid M-mode-like OCT imaging of three-dimensional microvasculature in vivo using reference-free processing of complex valued B-scans. Opt Lett. 2015; 40 (7): 1472–5.
20. Rogowska J, Patel N, Plummer S, Brezinski ME. Quantitative optical coherence tomographic elastography: method for assessing arterial mechanical properties. Br J Radiol. 2006; 79 (945): 707–11.
21. Song S, Huang Z, Nguyen TM, Wong EY, Arnal B, O'Donnell M, et al. Shear modulus imaging by direct visualization of propagating shear waves with phase-sensitive optical coherence tomography. J Biomed Opt. 2013; 18 (12): 121509.
22. Adie SG, Kennedy BF, Armstrong JJ, Alexandrov SA, Sampson DD. Audio frequency in vivo optical coherence elastography. Phys Med Biol. 2009; 54 (10): 3129–39.
23. Jonathan E, Enfield J, Leahy MJ. Correlation mapping method for generating microcirculation morphology from optical coherence tomography (OCT) intensity images. J Biophotonics. 2011; Sep; 4 (9): 583–7.
24. Jung Y, Dziennis S, Zhi Z, Reif R, Zheng Y, Wang RK. Tracking Dynamic Microvascular Changes during Healing after Complete Biopsy Punch on the Mouse Pinna Using Optical Microangiography. PLoS ONE. 2013; 8 (2): e57976.
25. Li H, Standish BA, Mariampillai A, Munce NR, Mao Y, Chiu S, et al. Feasibility of Interstitial Doppler Optical Coherence Tomography for In Vivo Detection of Microvascular Changes During Photodynamic Therapy. Lasers Surg Med. 2006; Sep 1; 38 (8): 754–61.
26. Standish BA, Lee KKC, Jin X, Mariampillai A, Munce NR, Wood MFG, et al. Interstitial Doppler Optical Coherence Tomography as a Local Tumor Necrosis Predictor in Photodynamic Therapy of Prostatic Carcinoma: An In vivo Study. Cancer Res. 2008; Dec 1; 68 (23): 9987–95.
27. Standish BA, Yang VX, Munce NR, Wong Kee Song LM, Gardiner G, Lin A, et al. Doppler optical coherence tomography monitoring of microvascular tissue response during photodynamic therapy in an animal model of Barrett's esophagus. Gastrointest Endosc. 2007; 66 (2): 326–33.
28. Hamdoon Z, Jerjes W, Upile T, Hopper C. Optical coherence tomography-guided photodynamic therapy for skin cancer: case study. Photodiagnosis Photodyn Ther. 2011; 8 (1): 49–52.
29. Themstrup L, Banzhaf CA, Mogensen M, Jemec GB. Optical coherence tomography imaging of non-melanoma skin cancer undergoing photodynamic therapy reveals subclinical residual lesions. Photodiagnosis Photodyn Ther. 2014; 11 (1): 7–12.

Литература

1. Casas A, Di Venosa G, Hasan T, Al Batlle. Mechanisms of resistance to photodynamic therapy. Curr Med Chem. 2011; 18 (16): 2486–515.
2. Mallidi S, Watanabe K, Timerman D, Schoenfeld D, Hasan T. Prediction of Tumor Recurrence and Therapy Monitoring Using Ultrasound-Guided Photoacoustic Imaging. Theranostics. 2015 Jan 1; 5 (3): 289–301.
3. Huang D, Swanson EA, Lin CP, Schuman S, Stinson WG, Chang W, et al. Optical coherence tomography. Science. 1991 Nov 22; 254 (5035): 1178–81.
4. Schmitt JM, Xiang SH. Cross-polarized backscatter in optical coherence tomography of biological tissue. Opt Lett. 1998 Jul 1; 23 (13): 1060–2.
5. Bouma BE, Tearney GJ. Clinical imaging with optical coherence tomography. Acad Radiol. 2002 Aug; 9 (8): 942–53.
6. Zagaynova EV, Gladkova ND, Shakhova NM, Streltsova OS, Kuznetsova IA, Yanvareva IA, et al. Optical Coherence Tomography Monitoring of Surgery in Oncology. В книге: Popp J, Tuchin V, Chiou A, Heinemann SH, editors. Handbook of Biophotonics. Wiley-VCH; 2012. p. 337–76.
7. Enfield J, Jonathan E, Leahy M. In vivo imaging of the microcirculation of the volar forearm using correlation mapping optical coherence tomography (cmOCT). Biomed Opt Express. 2011; 2 (5): 1184–93.
8. Mariampillai A, Leung MK, Jarvi M, Standish BA, Lee K, Wilson BC, et al. Optimized speckle variance OCT imaging of microvasculature. Opt Lett. 2010; 35 (8): 1257–9.
9. Kennedy BF, Hillman TR, McLaughlin RA, Quirk BC, Sampson DD. In vivo dynamic optical coherence elastography using a ring actuator. Opt Express. 2009; 17 (24): 21762–72.
10. Wang S, Li J, Manapuram RK, Menodiado FM, Ingram DR, Twa MD, et al. Noncontact measurement of elasticity for the detection of soft-tissue tumors using phase-sensitive optical coherence tomography combined with a focused air-puff system. Opt Lett. 2012; 37 (24): 5184–6.
11. Srivastava A, Verma Y, Rao K, Gupta P. Determination of elastic properties of resected human breast tissue samples using optical coherence tomographic elastography. Strain. 2011; Feb 1; 47 (1): 75–87.
12. Kennedy KM, McLaughlin RA, Kennedy BF, Tien A, Latham B, Saunders CM, et al. Needle optical coherence elastography for the measurement of microscale mechanical contrast deep within human breast tissues. J Biomed Opt. 2013; 18 (12): 121510.
13. Kennedy BF, McLaughlin RA, Kennedy KM, Chin L, Wijesinghe P, Curatolo A, et al. Investigation of Optical Coherence Micro-elastography as a Method to Visualize Cancers in Human Breast Tissue. Cancer Res. 2015; 75 (16): 3236–45.
14. Wang S, Larin KV, Li J, Vantipalli S, Manapuram RK, Aglyamov S, et al. A focused air-pulse system for optical-coherence-tomography-based measurements of tissue elasticity. Laser Physics Letters. 2013; 10 (7): 075605.
15. Nguyen TM, Song S, Arnal B, Wong EY, Huang Z, Wang RK, et al. Shear wave pulse compression for dynamic elastography using phase-sensitive optical coherence tomography. J Biomed Opt. 2014; 19 (1): 016013.
16. Zaitsev VY, Matveyev AL, Matveev LA, Gelikonov GV, Gubarkova EV, Gladkova ND, et al. Hybrid method of strain estimation in optical coherence elastography using combined sub-wavelength phase measurements and supra-pixel displacement tracking. J Biophotonics. 2016; 9 (5): 499–509.
17. Gubarkova EV, Dudenkova VV, Feldchtein FI, Timofeeva LB, Kiseleva EB, Kuznetsov SS, et al. Multi-modal optical imaging characterization of atherosclerotic plaques. J Biophotonics. 2015 Nov 25. doi: 10.1002/jbio.201500223.
18. Kiseleva E, Kirillin M, Feldchtein F, Vitkin A, Sergeeva E, Zagaynova E, et al. Differential diagnosis of human bladder mucosa pathologies in vivo with cross-polarization optical coherence tomography. Biomed Opt Express. 2015; Apr 1; 6 (4): 1464–76.
19. Matveev LA, Zaitsev VYu, Gelikonov GV, Matveyev AL, Moiseev AA, Ksenofontov SYu, et al. Hybrid M-mode-like OCT imaging of three-dimensional microvasculature in vivo using reference-free processing of complex valued B-scans. Opt Lett. 2015; 40 (7): 1472–5.
20. Rogowska J, Patel N, Plummer S, Brezinski ME. Quantitative optical coherence tomographic elastography: method for assessing arterial mechanical properties. Br J Radiol. 2006; 79 (945): 707–11.
21. Song S, Huang Z, Nguyen TM, Wong EY, Arnal B, O'Donnell M, et al. Shear modulus imaging by direct visualization of propagating shear waves with phase-sensitive optical coherence tomography. J Biomed Opt. 2013; 18 (12): 121509.
22. Adie SG, Kennedy BF, Armstrong JJ, Alexandrov SA, Sampson DD. Audio frequency in vivo optical coherence

elastography. Phys Med Biol. 2009; 54 (10): 3129–39.
23. Jonathan E, Enfield J, Leahy MJ. Correlation mapping method for generating microcirculation morphology from optical coherence tomography (OCT) intensity images. J Biophotonics. 2011; Sep; 4 (9): 583–7.
24. Jung Y, Dziennis S, Zhi Z, Reif R, Zheng Y, Wang RK. Tracking Dynamic Microvascular Changes during Healing after Complete Biopsy Punch on the Mouse Pinna Using Optical Microangiography. PLoS ONE. 2013; 8 (2): e57976.
25. Li H, Standish BA, Mariampillai A, Munce NR, Mao Y, Chiu S, et al. Feasibility of Interstitial Doppler Optical Coherence Tomography for In Vivo Detection of Microvascular Changes During Photodynamic Therapy. Lasers Surg Med. 2006; Sep 1; 38 (8): 754–61.
26. Standish BA, Lee KKC, Jin X, Mariampillai A, Munce NR, Wood MFG, et al. Interstitial Doppler Optical Coherence Tomography as a Local Tumor Necrosis Predictor in Photodynamic Therapy of Prostatic Carcinoma: An In vivo Study. Cancer Res. 2008; Dec 1; 68 (23): 9987–95.
27. Standish BA, Yang VX, Munce NR, Wong Kee Song LM, Gardiner G, Lin A, et al. Doppler optical coherence tomography monitoring of microvascular tissue response during photodynamic therapy in an animal model of Barrett's esophagus. Gastrointest Endosc. 2007; 66 (2): 326–33.
28. Hamdoon Z, Jerjes W, Upile T, Hopper C. Optical coherence tomography-guided photodynamic therapy for skin cancer: case study. Photodiagnosis Photodyn Ther. 2011; 8 (1): 49–52.
29. Themstrup L, Banzhaf CA, Mogensen M, Jemec GB. Optical coherence tomography imaging of non-melanoma skin cancer undergoing photodynamic therapy reveals subclinical residual lesions. Photodiagnosis Photodyn Ther. 2014; 11 (1): 7–12.